Chinese Chemical Letters 35 (2024) 109560

Contents lists available at ScienceDirect

Chinese Chemical Letters

journal homepage: www.elsevier.com/locate/cclet

Single nanozyme-based colorimetric biosensor for dopamine with enhanced selectivity *via* reactivity of oxidation intermediates

Caixia Zhu, Qing Hong, Kaiyuan Wang, Yanfei Shen*, Songqin Liu, Yuanjian Zhang*

Jiangsu Engineering Laboratory of Smart Carbon-Rich Materials and Devices, Jiangsu Province Hi-Tech Key Laboratory for Bio-Medical Research, School of Chemistry and Chemical Engineering, Medical School, Southeast University, Nanjing 211189, China

ARTICLE INFO

Article history:
Received 3 November 2023
Revised 4 January 2024
Accepted 22 January 2024
Available online 1 February 2024

Keywords:
Nanozyme
Colorimetry
Selectivity
Dopamine
Artificial recognition

ABSTRACT

Reliable and selective sensing of dopamine (DA) is essential for early diagnosis of mental diseases. Among the various potential methods, nanozyme-based sensing systems have demonstrated promising sensitivity and reliability. However, owing to the lack of substrate specificity, it is challenging to selectively detect DA using nanozymes. Herein, based on the reactivity of the DA oxidation intermediates, we report a cascade colorimetric sensing system for the selective detection of DA using only a single nanozyme. It was disclosed that the oxidation product of DA catalyzed by Co-N-doped carbon sheets (Co-N-C, a common oxidase-like nanozyme), dopamine quinone (DAQ), showed significant biocatalytic electron-donating activity in the reduction of O_2 to generate $O_2^{\bullet-}$. Further using $O_2^{\bullet-}$ to oxidize 3,3′,5,5′-tetramethylbenzidine (TMB), a colorimetric sensing platform for DA was constructed with a linear detection range of 50 nmol/L to 50 μmol/L and a low limit of detection of 4 nmol/L. Thanks to the reactivity of the oxidation product, without any biometric units (such as nucleic acids, enzymes, and antibodies/antigens), the reaction selectivity of DA against other interferences (*e.g.*, ascorbic acid, adrenaline, 5-hydroxytryptamine, and glutathione) was enhanced up to 71-fold. Beyond complicated cascade systems requiring at least two nanozymes, sophisticated artificial recognition *via* multiple interactions was simplified by exploiting the oxidative properties of product intermediates; thus, only a single common oxidase-like nanozyme was needed. This work offers a new strategy to enhance the selectivity of nanozymes for bioanalytical applications.

Dopamine (DA) is a representative monoamine neurotransmitter that plays a fundamental role in the function of the human central nervous system [1–4]. The abnormal DA levels are closely related to schizophrenia, Alzheimer's disease, Parkinson's disease, pheochromocytoma, and paraganglioma [5–8]. Therefore, the accurate and reliable measurement of DA in body fluids, such as blood, cerebrospinal fluid, and urine, is of great importance in clinical diagnosis [9–13]. To date, many techniques have been developed for sensitive and selective detection of DA, including colorimetry [14–16], fluorescence [17–19], electrochemiluminescence [20,21] and electrochemistry [22–25]. Among them, colorimetric techniques have been widely concerned in recent years due to their advantages of simple operational techniques and low cost [26–29]. Traditional colorimetric biosensors of dopamine are mostly based on the binding ability of dopamine on DNA sequence that prevents the DNA sequence adsorption on gold nanoparticles (AuNPs) [12,15,30,31]. The unprotected AuNPs then aggregate and turn blue upon addition of salt. However, this method suffers significantly from poor stability of DNA and AuNPs. Therefore, it is highly desirable to develop efficient and reliable colorimetric sensors composed of stable sensing elements.

Nanozymes are a class of nanomaterials with enzyme-like activity. They have attracted intensive attention because of their high stability and catalytic activities [32–37]. Nanozyme-based colorimetric sensors have been explored to detect DA with promising sensitivity and reliability by using the inhibitory effect of DA on the catalytic oxidation reaction of nanozymes [16,28,38-41]. However, neurotransmitters (*e.g.*, adrenaline and serotonin) and biological small molecules (*e.g.*, ascorbic acid) coexist with DA, making selective detection of DA highly challenging [42,43]. Along this line, the development of robust nanozyme-based biosensors for colorimetric detection of DA with high selectivity is highly envisioned.

Over the past few years, several strategies have been explored to improve the selectivity of nanozymes, including sophisticated control of nanozyme structures and surfaces (*e.g.*, molecular imprinting [44], coordination regulation [45], amino acid func-

* Corresponding authors.
E-mail addresses: Yanfei.Shen@seu.edu.cn (Y. Shen), Yuanjian.Zhang@seu.edu.cn (Y. Zhang).

https://doi.org/10.1016/j.cclet.2024.109560
1001-8417/

tionalization [46]) and the collaboration of additional recognition elements (*e.g.*, aptamer, enzymes, and antibodies/antigens) [47,48]. Our group proposed a cascade strategy to improve the reaction selectivity [49]. It relied on the operation principle that not all the biocatalytic products of the prior nanozyme is the substrates for the subsequent nanozymes. Along this line, the rational selection of nanozymes with appropriate activities and sequences for ingenious nanozyme cascades is key. Recently, inspired by cellular metabolism networks, we further developed a cascade nanozymatic network with diverse responses to a single stimulus to achieve highly selective reactions [50]. In fact, both intrinsic control of structures and surfaces and extrinsic biomimetic approaches improve selectivity, essentially by multiple interactions with substances. Notably, the reaction selectivity of the nanozyme system could be improved by the gradual screening of substrates; at the same time, however, it also requires more building units, which would increase complexity of biocatalytic systems as well as uncontrollable factors. Therefore, to improve the reaction selectivity of nanozymes, it is desirable to realize multiple interactions between the nanozymes and substrates as simply as possible.

Herein, based on the reactivity of DA oxidation intermediates, we report a cascade colorimetric sensing system for DA with a high reaction selectivity using only a single nanozyme. We found that the oxidation product of DA catalyzed by Co-N-doped carbon sheets (Co-N-C) with oxidase-like activity, dopamine quinone (DAQ), had significant biocatalytic electron-donating activity in the reduction of O_2 to generate $O_2^{\bullet-}$. The resulting $O_2^{\bullet-}$ further oxidized 3,3′,5,5′-tetramethylbenzidine (TMB), outputting a quantifiable analytical signal of absorbance equivalent to DA in the concentration range of 50 nmol/L to 50 μmol/L with a lower limit of detection of 4 nmol/L. Notably, without any biometric units (such as nucleic acids, enzymes, and antibodies/antigens), compared to other interferences (*e.g.*, ascorbic acid, adrenaline, 5-hydroxytryptamine, and glutathione) whose oxidation products has negligible activities, the reaction selectivity of DA was enhanced up to 71-fold.

Owing to their outstanding enzyme-like activity and ease of synthesis, Co-N-doped carbon sheets (Co-N-C) were used as representative oxidase-like nanozymes to oxidize DA. According to a previously reported method, the Co-N-C nanozyme was prepared using a salt-template method [51]. As shown in Fig. S1a (Supporting information), the synthesized Co-N-C exhibited an ultrathin nanosheet morphology. Energy-dispersive X-ray spectroscopy (EDS) mapping demonstrated a uniform distribution of elemental carbon, nitrogen, and cobalt, without any evident phase separation (Fig. S1b in Supporting information). This was in agreement with the literature [51], indicating the successful synthesis of Co-N-C nanozymes. The oxidase-like catalytic activity of Co-N-C was investigated using molecular O_2 and DA as the substrates. The time evolution of the UV−vis absorption spectra of DA in the presence of Co-N-C is shown in Fig. 1a. Upon the addition of Co-N-C, an absorption maximum appeared at 395 nm, corresponding to the yellow chromophore dopamine quinone (DAQ). This demonstrated the significant oxidase-like activity of Co-N-C.

Interestingly, we found that the oxidation product of DA had a strong oxidizing ability for TMB. To avoid interference from Co-N-C, it was removed by filtration and the supernatant of DA_{ox} was denoted as DA_{ox}. As shown in Fig. 1b, a typical blue product of TMB_{ox} appeared, indicating that DA_{ox} had an oxidation ability. To understand the intrinsic essence of the phenomenon, DA and DA_{ox} in solution were first measured using electrospray ionization mass spectrometry (ESI-MS). Prior to oxidation, a fragment of DA ([M + H]) was observed at *m/z* 154.1 (Fig. 1c, top panel). Two oxidation product fragments (*m/z* 152.1 and 150.1) were observed after oxidation using the Co-N-C nanozyme (Fig. 1c, bottom panel). This demonstrated that the reaction of DA oxidation catalyzed

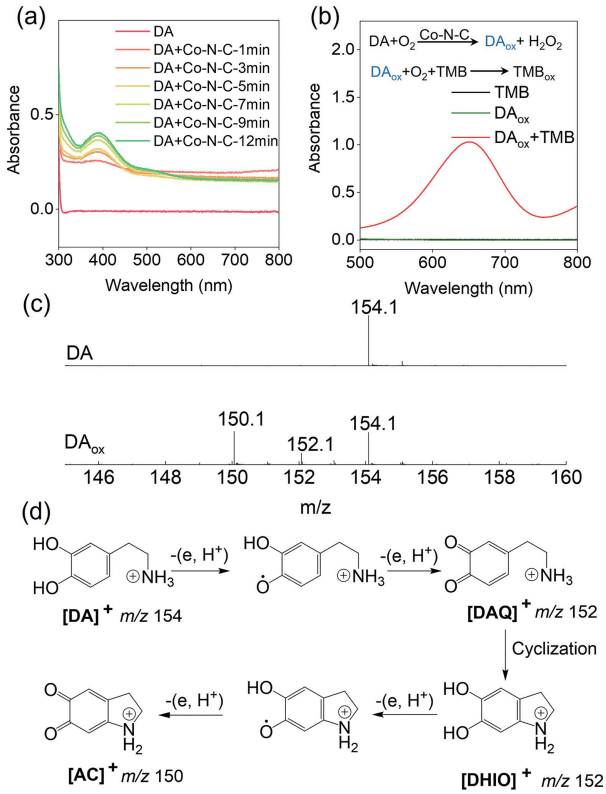

Fig. 1. Dopamine oxidase-like activity of Co-N-C nanozymes. (a) UV−vis absorption spectra of DA (10 mmol/L) catalyzed by Co-N-C (0.05 mg/mL) in HAc-NaAc (0.1 mol/L, pH 3.5) buffer solution. (b) UV−vis absorption spectra of TMB (0.5 mmol/L) with DA_{ox} (oxidation product of DA). (c) ESI-MS spectra of DA and DA_{ox}. (d) Reaction pathway of DA oxidation catalyzed by Co-N-C.

by Co-N-C followed the mechanism of gradual dehydrogenation (Fig. 1d). Meanwhile, H_2O_2 as the oxygen reduction product of O_2, was also confirmed by TMB-HRP chromatography (Fig. S2 in Supporting information).

To understand the composition of the DA_{ox} solution, the time evolution of the UV−vis absorption spectra of the DA_{ox} solution was monitored after removing the Co-N-C nanozyme. As shown in Fig. 2a, the absorbance of DAQ ($\lambda = 395$ nm) decreased with time, whereas that of aminochrome (AC, $\lambda = 300$ nm and 475 nm), the oxidation product of DA losing four hydrogen atoms, increased. Accordingly, after removing Co-N-C and standing for different time (*i.e.*, 3, 7, 15, 30, 50, and 90 min), the oxidation ability of the DA_{ox} solution for TMB gradually decreased with time (Fig. 2b). Therefore, it was reasonable to speculate that the number of oxidative species in the DA_{ox} solution gradually decreased with time. To confirm this hypothesis, a DA_{ox} solution with no oxidation ability was prepared by a 120 min standing operation. Co-N-C nanozymes were added to the DA_{ox} solution and catalyzed the previously unreacted DA. Co-N-C was then removed by filtration after incubation for 10 min. As shown in Fig. S3 (Supporting information), the newly obtained DA_{ox} solution regained its ability to oxidize TMB to TMB_{ox}. These control results suggested that the oxidation ability of the DA_{ox} solution was derived from the new product, but it was unstable.

The involvement of oxidative stress and the production of reactive oxygen species has been reported in neurodegenerative disorders [52,53]. A possible source of oxidative stress is the redox reactions that specifically involve DA. Specifically, spontaneous oxidation of DA in the presence of molecular oxygen leads to the formation of several cytotoxic molecules, including superoxide

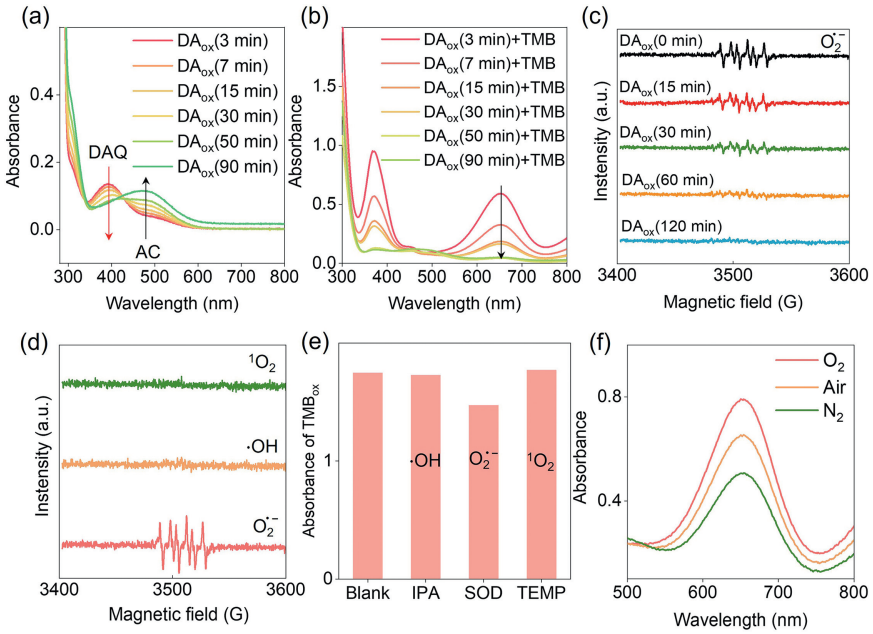

Fig. 2. Mechanism of the oxidation of TMB in DA_{ox} solution. (a) Time evolution of the UV–vis absorption spectra of DA_{ox} after removal of Co-N-C. DA: 10 mmol/L, HAc-NaAc buffer solution (pH 3.5): 0.1 mol/L. (b) UV–vis absorption spectra of TMB (0.5 mmol/L) after reaction with DA_{ox} solution standing for different time (3 min, 7 min, 15 min, 30 min, 50 min, and 90 min). (c) ESR spectra of the spin adducts of $O_2^{\bullet-}$ of DA_{ox} solution standing for different time of 0 min, 15 min, 30 min, 60 min, and 120 min. (d) ESR spectra of singlet oxygen, hydroxyl radical, and superoxide radical-trapping agent adducts. (e) Effects of ROS scavengers on the oxidation efficiency of TMB with DA_{ox} based on the typical absorption at 652 nm (TMB_{ox}). (f) UV–vis spectra of TMB in DA_{ox} solution saturated with O_2, air, and N_2.

anion free radicals ($O_2^{\bullet-}$), hydroxyl radicals ($^{\bullet}OH$) and reactive quinone [54–57]. To monitor possible intermediate reactive oxygen species (ROS), electron spin resonance (ESR) spectra were measured. As shown in Fig. 2c, using 5,5-dimethyl-1-pyrroline *N*-oxide (DMPO) as the spin-trapping agent, a typical ESR signal corresponding to the adduct of DMPO with a superoxide anion radical (DMPO-$O_2^{\bullet-}$) was observed. The ESR spectra shown in Fig. 2d demonstrated that there were no signals for $^{\bullet}OH$ or singlet oxygen-trapping agent adducts. Scavenger trapping was performed to further confirm the existence of $O_2^{\bullet-}$ in the DA_{ox} solution (Fig. 2e). Consistent with the phenomenon shown in Fig. 2b, the ESR signal of DMPO-$O_2^{\bullet-}$ decreased with increasing DA_{ox} standing time (Fig. 2c). These results confirmed that the $O_2^{\bullet-}$ intermediate was the main source of the oxidation ability of the DA_{ox} solution.

Subsequently, the source of $O_2^{\bullet-}$ in the DA_{ox} solution was explored. Because of the very short lifetime of $O_2^{\bullet-}$ in aqueous solution [58,59], $O_2^{\bullet-}$ was most likely derived from the internal reaction of the DA_{ox} solution rather than the Co-N-C catalyzed DA oxidation reaction. Therefore, it is necessary to explore the reaction in the DA_{ox} solution after removal of the Co-N-C nanozyme. As shown in Fig. 2a, the conversion of DAQ, one dehydrogenation product of DA ($\lambda = 395$ nm), to another product AC ($\lambda = 300$ nm and 475 nm) was observed, in view of the change in the solution absorption peaks. According to previous reports, DAQ has the electron-donating ability to donate electrons to O_2 to generate reactive oxygen species [60]. To verify this claim, a series of control experiments were performed. Three aliquots of the DA_{ox} solution were saturated with O_2, air, and N_2 to simulate the reaction environments with different oxygen concentrations. TMB was then introduced into each solution and incubated for 1 min. Finally, the absorption of the solutions was measured. As shown in Fig. 2f, the absorbance of TMB_{ox} increased with the oxygen concentration, indicating that the increase in O_2 concentration favored the production of $O_2^{\bullet-}$ in the DA_{ox} solution. These results suggested that the $O_2^{\bullet-}$ of the DA_{ox} solution was mainly derived from the pro-oxidant effect of DAQ, which donates electrons to O_2 to generate $O_2^{\bullet-}$. To further confirm this assumption, additional control experiments were performed (Fig. S4a in Supporting information). The DA_{ox} solution (DA_{ox}, *hv*) was obtained by irradiating the DA solution with full light (300 mW/cm^2). When TMB was introduced into the DA_{ox} (*hv*) solution, no blue product (TMB_{ox}) was formed. The ESR spectra in Fig. S4b (Supporting information) demonstrated that there were no signals for the superoxide radical-trapping agent adducts. Moreover, the absorbance of DA_{ox} (*hv*) did not change with time (Fig. S4c in Supporting information), and only one fragment of DA_{ox} (*hv*) was observed at *m/z* 150.1 (Fig. S4d in Supporting information), indicating that the product of DA upon irradiation was AC rather than DAQ. It was further demonstrated that $O_2^{\bullet-}$ originates from DAQ, which had electron-donating ability.

As an oxidase-like nanozyme, Co-N-C exhibited low reaction selectivity. For example, adrenaline (AH), a common interference of DA, can also be catalytically oxidized by Co-N-C to produce AH_{ox} and H_2O_2 (Figs. S5a and S6a in Supporting information). However, in the absence of other enzymes (*e.g.*, HRP), AH_{ox} could not react with TMB to produce the targeted TMB_{ox} because of the intermediate screening effect (Fig. S5b in Supporting information). 5-Hydroxytryptamine (5-HT), another typical interference of DA, was used as a control substrate. As shown in Figs. S5a and S6b (Supporting information), the catalytic effect of Co-N-C on the oxidation of 5-HT was negligible. As shown in Fig. S5b, TMB_{ox} was not generated during the final reaction. Therefore, among the above three typical substrates, only DA could be screened to generate the final product TMB_{ox} (Fig. 3a and Fig. S5b). In other words, the selectivity of a nanozyme system can be substantially improved by rational design based on the properties of the intermediates. In addition, the same selectivity enhancement can be realized when Co-N-C was replaced by other oxidase-like nanozymes (*e.g.*, Co-N-CNTs, Co-N-CNPs, Fe-N-C, and Pt-C; Fig. S7 in Supporting information).

Notably, in contrast to the previous cascade system that required critical selection of nanozymes with appropriate activities and sequences, sophisticated artificial recognition *via* multiple interactions was simplified by exploiting the oxidative properties of preliminary oxidation products; thus, only a single common

Table 1
Comparison of the enhanced folds of selectivity for DA *via* different detection methods.[a]

Method	Interference	Relative folds of selectivity	Ref.
Molecularly imprinted	AA	1.6	[61]
DBA-aptachip$_{bPEI}$	AA	17	[62]
Au/RP1/Ni_3HHTP_2 microelectrode	5-HT	29	[2]
Anti-DA aptamer	5-HT	2.6	[63]
AptCFE	AA	10.6	[10]
GO	Cysteine	4.3	[64]
In_1-N-C	Cysteine	1.8	[25]
Cu-BTA-COF platform	AA	7.2	[16]
Ru1-labeled anti-DA aptamer	5-HT	5	[21]
Stepwise substrate screening	5-HT	71	This work

[a] The relative fold of reaction selectivity was calculated by dividing the signal of the probe for DA by the signal of the probe for interference.

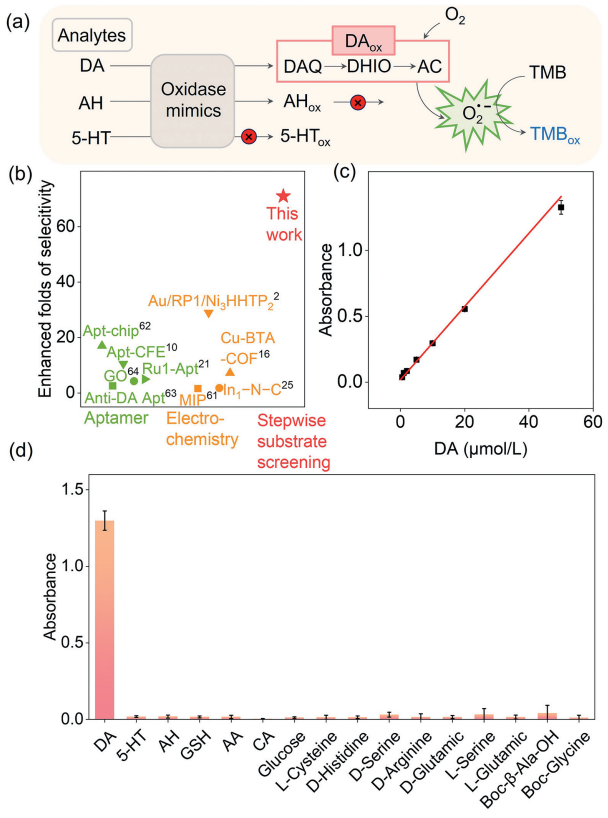

Fig. 3. Selectivity enhancement of DA detection using oxidation-product reactivity in a single oxidase-like nanozyme system. (a) Scheme of DA selective detection mechanism based on stepwise substrate screening assisted by the transition from DAQ to AC during DA oxidation. (b) Comparison of the enhanced folds of selectivity for DA using different methods with various sensing elements. The superscript number represent the reference numbers in Table 1. (c) Calibration curves for DA detection using a single Co-N-C nanozyme and DA oxidation product reactivity. (d) Absorbance of TMB$_{ox}$ produced by the oxidation product of DA and other small molecules as potential interference.

oxidase-like nanozyme was needed. Therefore, the same selectivity principle could be extended to other nanozymatic reactions with reasonable design. In contrast to our previous reports [49,50], the as-developed sensor could be designed with fewer constraints and was more generalizable. As can be seen in Fig. 3b, without any complex modification of nanozymes and any introduction of biorecognition elements, the relative reaction selectivity of DA against 5-HT was up to 71-fold. The enhanced selectivity for DA based on the nanozymatic system significantly surpassed that of previously reported DA sensors (Fig. 3b; see Table 1 for more details) [61–64]. This showed that beyond meticulous control of the structure and surface (*e.g.*, molecular imprinting [44], coordination regulation [45], and amino acid functionalization [46]) and the combination of nanozymes with natural enzymes [48], a nanozymatic system that learns principles from metabolism can also achieve selective enhancement of nanozyme systems.

Table 2
DA recovery assay in normal human serum samples.

Added DA (μmol/L)	Found (μmol/L)	Recovery rate
0.05	0.048	97%
6	6.0	100%
20	19.4	97%
50	49.3	98%

Next, the potential application of this strategy for DA detection was demonstrated. Under optimal reaction conditions (Fig. S8 in Supporting information), the absorbance of TMB$_{ox}$ at 652 nm increased linearly with an increase in DA concentration in the range of 50 nmol/L–50 μmol/L (Fig. 3c). The calculated limit of detection (LOD) of DA was 4 nmol/L at S/N = 3, which is superior to or compatible with many previously reported DA-sensing reactions (Table S1 in Supporting information). In addition, the selectivity of the established DA detection system was verified by a dozen of interferences including ascorbic acid (AA), AH, 5-HT, glutathione (GSH), glucose, citric acid (CA), L-Cys, D-His, D-Ser, D-Arg, D-Glu, L-Ser, L-Glu, Boc-β-Ala-OH, and Boc-Glycine. As shown in Fig. 3d, only DA caused intense signal changes in the developed platform, demonstrating excellent selectivity for DA detection. The detection of DA in the human serum was further explored to evaluate the practical applicability of the colorimetric sensor. As shown in Table 2, a high recovery rate was obtained for DA detection in diluted human serum (0.05, 6, 20, and 50 μmol/L), indicating its practicability for real sample detection. Therefore, highly selective DA sensors were successfully constructed using stable sensing elements that were consistent with only one nanozyme. It would be attractive to build DA sensors with high stability and low cost for practical applications because of the absence of fragile biological components.

In summary, based on the different reactivities of the oxidation products, we developed a cascade colorimetric sensing system for the selective and reliable detection of DA against a diverse range of interferences using only a single conventional oxidase-like nanozyme. The oxidation product of DA catalyzed by Co-N-C, dopamine quinone (DAQ), showed significant biocatalytic electron-donating activity in the reduction of O_2 to generate $O_2^{\bullet-}$. Further using the intermediate $O_2^{\bullet-}$ to oxidize TMB, a colorimetric sensing platform was constructed for DA with a linear detection range of 50 nmol/L to 50 μmol/L and a low limit of detection of 4 nmol/L. More importantly, without any natural biometric units (*e.g.*, aptamer, enzymes, and antibodies/antigens), the reaction selectivity of DA was enhanced up to 71-fold and making DA stand out from a dozen of interferences, including AA, AH, 5-HT, GSH, glucose, CA, L-Cys, D-His, D-Ser, D-Arg, D-Glu, L-Ser, L-Glu,

Boc-β-Ala-OH, and Boc-Gly. Notably, beyond the previous cascade system that required critical selection of nanozymes with appropriate activities and sequences, sophisticated artificial recognition *via* multiple interactions was simplified by exploiting the oxidative properties of preliminary oxidation products; thus, only a single common oxidase-like nanozyme was needed. This work offers a new direction for the design of nanozymatic bioanalytical sensors with enhanced selectivity.

Declaration of competing interest

The authors declare that they have no known competing financial interests or personal relationships that could have appeared to influence the work reported in this paper

Acknowledgment

This work was supported by the National Natural Science Foundation of China (Nos. 22174014 and 22074015).

Supplementary materials

Supplementary material associated with this article can be found, in the online version, at doi:10.1016/j.cclet.2024.109560.

References

[1] A. Usiello, J.H. Baik, F. Rougé-Pont, et al., Nature 408 (2000) 199–203.
[2] Y. Wang, Y. Qian, L. Zhang, et al., J. Am. Chem. Soc. 145 (2023) 2118–2126.
[3] Y. He, I. Kaya, R. Shariatgorji, et al., Nat. Commun. 14 (2023) 5804.
[4] A.C. Krok, M. Maltese, P. Mistry, et al., Nature 621 (2023) 543–549.
[5] D. Aarsland, L. Batzu, G.M. Halliday, et al., Nat. Rev. Dis. Primers 7 (2021) 47.
[6] X. Zhang, D. Tsuboi, Y. Funahashi, et al., Int. J. Mol. Sci. 23 (2022) 11643.
[7] V. Cesaroni, F. Blandini, S. Cerri, Expert Opin. Ther. Targets 26 (2022) 837–851.
[8] A.F. Khan, Q. Adewale, S. Lin, et al., Nat. Commun. 14 (2023) 6009.
[9] F. Sun, J. Zeng, M. Jing, et al., Cell 174 (2018) 481–496.
[10] H. Hou, Y. Jin, H. Wei, et al., Angew. Chem. Int. Ed. 59 (2020) 18996–19000.
[11] R.P. Shukla, M. Aroosh, A. Matzafi, H. Ben-Yoav, Adv. Funct. Mater. 31 (2021) 2004146.
[12] X. Liu, J. Liu, View 2 (2021) 20200102.
[13] J. Li, Y. Liu, L. Yuan, et al., Nature 606 (2022) 94–101.
[14] H. Li, H. Lin, X. Wang, W. Lv, F. Li, ACS Appl. Mater. Interfaces 11 (2019) 36469–36475.
[15] X. Liu, F. He, F. Zhang, et al., Anal. Chem. 92 (2020) 9370–9378.
[16] J. Yue, L. Song, Y. Wang, et al., Anal. Chem. 94 (2022) 14419–14425.
[17] X. Liu, Y. Hou, S. Chen, J. Liu, Biosens. Bioelectron. 173 (2021) 112798.
[18] F. Qu, Z. Guo, D. Jiang, X.E. Zhao, Chin. Chem. Lett. 32 (2021) 3368–3371.
[19] A.G. Salinas, J.O. Lee, S.M. Augustin, et al., Nat. Commun. 14 (2023) 5915.
[20] F.A. Bushira, S.A. Kitte, C. Xu, et al., Anal. Chem. 93 (2021) 9949–9957.
[21] D. Zhang, M. Qian, X. Yang, et al., Anal. Chem. 95 (2023) 5500–5506.
[22] X. Xie, D.P. Wang, C. Guo, et al., Anal. Chem. 93 (2021) 4916–4923.
[23] M.A. Ali, C. Hu, B. Yuan, et al., Nat. Commun. 12 (2021) 7077.
[24] D. Sen, R.A. Lazenby, Anal. Chem. 95 (2023) 6828–6835.
[25] R. Li, W. Guo, Z. Zhu, et al., Anal. Chem. 95 (2023) 7195–7201.
[26] Z. Li, J.R. Askim, K.S. Suslick, Chem. Rev. 119 (2018) 231–292.
[27] J. Zeng, Y. Zhang, T. Zeng, et al., Nano Today 32 (2020) 100855.
[28] R. Li, L. Fan, S. Chen, et al., ACS Appl. Mater. Interfaces 14 (2022) 55201–55216.
[29] Y. Fu, C. Du, Q. Zhang, et al., Anal. Chem. 94 (2022) 15040–15047.
[30] Y. Zheng, Y. Wang, X. Yang, Sens. Actuator. B 156 (2011) 95–99.
[31] Y. Zhang, S. Qi, Z. Liu, et al., Mater. Sci. Eng. C 61 (2016) 207–213.
[32] L. Gao, J. Zhuang, L. Nie, et al., Nat. Nanotechnol. 2 (2007) 577–583.
[33] W. Zhen, Y. Liu, W. Wang, et al., Angew. Chem. Int. Ed. 59 (2020) 9491–9497.
[34] L. Jiao, H. Yan, Y. Wu, et al., Angew. Chem. Int. Ed. 59 (2020) 2565–2576.
[35] D. Chao, Q. Dong, Z. Yu, et al., J. Am. Chem. Soc. 144 (2022) 23438–23447.
[36] G. Li, H. Liu, T. Hu, et al., J. Am. Chem. Soc. 145 (2023) 16835–16842.
[37] W. Liu, Y. Zhang, G. Wei, et al., Angew. Chem. Int. Ed. 62 (2023) e202304465.
[38] J. Zhu, X. Peng, W. Nie, et al., Biosens. Bioelectron. 141 (2019) 111450.
[39] S. Wang, Z.F. Hu, Q.L. Wei, et al., Nano Res. 15 (2022) 4266–4273.
[40] W. Fu, K. Zhang, X. Zhang, et al., Electrochim. Acta 437 (2023) 141535.
[41] Z. Wu, W. Liu, H. Lu, et al., Nanoscale 15 (2023) 13289–13296.
[42] M.N. Ivanova, E.D. Grayfer, E.E. Plotnikova, et al., ACS Appl. Mater. Interfaces 11 (2019) 22102–22112.
[43] X. Wang, G. Wei, W. Liu, et al., Anal. Chem. 95 (2023) 5937–5945.
[44] Z. Zhang, X. Zhang, B. Liu, J. Liu, J. Am. Chem. Soc. 139 (2017) 5412–5419.
[45] Y. Wang, G. Jia, X. Cui, et al., Chem 7 (2021) 436–449.
[46] Y. Zhou, H. Sun, H. Xu, et al., Angew. Chem. Int. Ed. 57 (2018) 16791–16795.
[47] Y. Ouyang, Y. Biniuri, M. Fadeev, et al., J. Am. Chem. Soc. 143 (2021) 11510–11519.
[48] C.B. Ma, Y. Xu, L. Wu, et al., Angew. Chem. Int. Ed. 61 (2022) e202116170.
[49] Q. Zhou, H. Yang, X. Chen, et al., Angew. Chem. Int. Ed. 61 (2021) e202112453.
[50] C. Zhu, Z. Zhou, X.J. Gao, et al., Chem. Sci. 14 (2023) 6780–6791.
[51] L. Jiao, J. Wu, H. Zhong, et al., ACS Catal. 10 (2020) 6422–6429.
[52] T.G. Hastings, D.A. Lewis, M.J. Zigmond, Proc. Natl. Acad. Sci. U. S. A. 93 (1996) 1956–1961.
[53] S. Chakrabarti, M. Bisaglia, Antioxidants 12 (2023) 955.
[54] D.G. Graham, S.M. Tiffany, W.R. Bell, W.F. Gutknecht, Mol. Pharmacol. 14 (1978) 644–653.
[55] J. Lotharius, P. Brundin, Nat. Rev. Neurosci. 3 (2002) 932–942.
[56] N.A. Mautjana, J. Estes, J.R. Eyler, A. Brajter-Toth, Electroanalysis 20 (2008) 1959–1967.
[57] Y. Song, G.R. Buettner, Free Radical Biol. Med. 49 (2010) 919–962.
[58] M. Hayyan, M.A. Hashim, I.M. AlNashef, Chem. Rev. 116 (2016) 3029–3085.
[59] S.F. Zhao, F.X. Hu, Z.Z. Shi, et al., Nano Res. 14 (2020) 879–886.
[60] H. Liu, X. Qu, H. Tan, et al., Acta Biomater. 88 (2019) 181–196.
[61] J. Yang, Y. Hu, Y. Li, Biosens. Bioelectron. 135 (2019) 224–230.
[62] T. Lin, K. Wei, S. Ju, C. Huang, H. Yang, J. Mater. Chem. B 6 (2018) 3387–3394.
[63] R. Li, D. Zhang, X. Li, H. Qi, Bioelectrochemistry 146 (2022) 108148.
[64] A. Teniou, A. Rhouati, G. Catanante, Appl. Biochem. Biotechnol. 194 (2022) 1925–1937.